Available online at www.sciencedirect.com
SCIENCE DIRECT®
Planetary and Space Science 52 (2004) 313–323
Planetary and Space Science
www.elsevier.com/locate/pss

Comet Hyakutake (C/1996 B2): Spectacular disconnection event and the latitudinal structure of the solar wind

M. Snow[a,*], J.C. Brandt[b], Y. Yi[a,1], C.C. Petersen[a,2], H. Mikuz[c]

[a] *Laboratory for Atmospheric and Space Physics, University of Colorado, Boulder, CO 80309, USA*
[b] *Institute for Astrophysics, Department of Physics and Astronomy, University of New Mexico, Albuquerque, NM 87131, USA*
[c] *Crni Vrh Observatory, Kersnikova 11, 1000 Ljubljana, Slovenia*

Received 9 September 2002; received in revised form 8 October 2003; accepted 14 October 2003

Abstract

Images of comet Hyakutake (C/1996 B2) are analyzed in conjunction with solar wind data from spacecraft to determine the relationship between solar wind conditions and plasma tail morphology. The disconnection event (DE) on March 25, 1996 is analyzed with the aid of data from the IMP-8 and WIND Earth-orbiting spacecraft and the DE is found to be correlated with a crossing of the heliospheric current sheet. The comet was within 0.1 AU of Earth at the time of the DE and data from IMP-8 and WIND show no high-speed streams, significant density enhancements or shocks.

The latitudinal variation in the appearance and orientation of the plasma tail are interpreted based on results from the Ulysses spacecraft. In the polar solar wind region, the comet has a relatively undisturbed appearance, no DEs were observed, and the orientation of the plasma tail was consistent with a higher solar wind speed. In the equatorial solar wind region, the comet's plasma tail had a disturbed appearance, a major DE was observed, and the orientation of the plasma tail was consistent with a lower solar wind speed. The boundary between the equatorial and polar regions crossed by comet Hyakutake in April 1996 was near 30°N (ecliptic) or 24°N (solar) latitude.

Keywords: Comets; Solar wind; Plasma tail; Disconnection events

1. Introduction

The *Ulysses* spacecraft has mapped the solar wind as a function of latitude (Phillips et al., 1995a, b; McComas et al., 1998) and showed that the polar region is distinctly different than the equatorial region sampled by all near-Earth instruments. In the well-studied equatorial region, the average solar wind speed is about 450 km s^{-1}, with an average proton = electron density of about 9 cm^{-3}. The speed and density in this region are highly variable. In the polar region sampled by *Ulysses*, the typical speed of the solar wind is greater, about 750 km s^{-1}. The density in the polar region is much lower ($\sim$ 3 cm^{-3}), and the speed and density of the solar wind at these latitudes are much more steady than in the equatorial zone. The boundary between the equatorial and polar regions is approximately determined by the maximum latitudinal extent of the heliospheric current sheet (HCS). This description applies to solar-minimum type conditions and is appropriate to the time of comet Hyakutake. It does not apply to times near solar maximum (Smith et al., 2001; McComas et al., 2002).

Cometary plasma tails are expected to show a related bimodal distribution in their appearance: at equatorial latitudes the plasma tail is disturbed and disconnection events (DEs) occur, but at polar latitudes the plasma tail appears smooth and no DEs are observed. The orientation of the plasma tail reflects the high solar wind speed in the polar region and low speed in the equatorial region. The plasma tail of comet de Vico (122P) was observed as the comet moved from heliocentric ecliptic latitude of 29.3°S to 56.9°N (heliographic latitude of 27.7°S to 55.1°N). The behavior of its plasma tail follows this simple paradigm (see Brandt et al., 1997b). This paradigm was described in Brandt and Snow (2000), where it was also shown to be consistent with historical data essentially for the entire 20th century. Gombosi et al. (1997)

* Corresponding author. Tel.: +1-303-735-2143; fax: +1-303-492-6444.
E-mail address: snow@lasp.colorado.edu (M. Snow).
[1] Now at Department of Astronomy and Space Science, Chungnam National University, Daejon 305-764, South Korea.
[2] Now at Loch Ness Productions, P.O. Box 256, Groton, MA 01450, USA.

0032-0633/$ - see front matter © 2003 Elsevier Ltd. All rights reserved.
doi:10.1016/j.pss.2003.10.001

have presented MHD simulations of comet Hale–Bopp for equatorial and polar solar-wind conditions.

In situ measurements obtained by *Ulysses* on May 1, 1996 have been interpreted as the signature of comet Hyakutake's plasma tail 550 million km from its nucleus. The signature appears in magnetic field data (Jones et al., 2000) and in ion composition measurements (Gloeckler et al., 2000). Detecting the plasma signature more than 3.8 AU from the nucleus is remarkable. The persistence of the signature was probably due to comet Hyakutake being in the steady polar solar wind during the time period of interest (see Figs. 3 and 11). For additional discussion, see Jones (2002) and Wegmann (2002).

2. Comet Hyakutake

On January 30, 1996, a dedicated amateur observer in Japan, Yuji Hyakutake, was scanning the skies with a pair of large binoculars. He was looking at comet 1995 Y1 which he had previously discovered, when he happened to come across a 11th magnitude object only a few degrees away from 1995 Y1. Just a few months later, this faint object became the "Great Comet of 1996".

Comet Hyakutake had a highly inclined orbit ($i = 124.9°$) and passed very close (≈ 0.1 AU) to the Earth in the Spring of 1996. Its path across the sky at nearly circumpolar declination was extremely favorable for observers everywhere in the northern hemisphere. The comet was very bright, and therefore a large number of wide field images were submitted to the Ulysses Comet Watch from amateur observers all over the world. We have made use of this excellent archive in the analysis presented here. The images which we have selected to illustrate the comet's plasma tail's behavior in this paper are listed in Appendix A.

3. Appearance

Much like comet de Vico, the overall appearance of Hyakutake's plasma tail varied over the course of its apparition. While the comet was in the polar region, the plasma tail was relatively smooth with no DEs. In the equatorial region, the plasma tail was highly disturbed, and one major DE was observed (cf. Section 5).

Fig. 1 shows sample observations of the comet in the polar region. Compare these images to the images of the comet in the equatorial region, Figs. 2 and 3 is a time sequence of images of the comet and shows the change in the plasma tail's appearance as the comet moves from the equatorial to the polar region. The change in appearance is entirely consistent with an equatorial–polar region boundary at 30°N (ecliptic) or 24°N (solar) latitude. Note that sequences of images taken with the same telescope (as in Fig. 3) are optimum for showing the transition between the equatorial and polar regions (Brandt and Snow 2000).

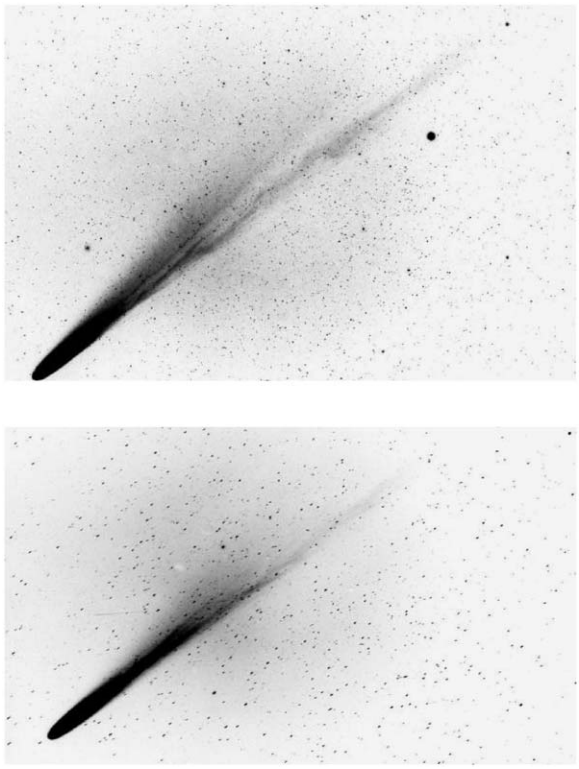

Fig. 1. Images of comet Hyakutake in the polar region of the solar wind showing a relatively undisturbed appearance. (Top) April 18.8, 1996, latitudes 33°N (ecliptic) and 26°N (heliographic); (Bottom) April 20.8, 1996, latitudes 36°N (ecliptic) and 29°N (heliographic). Compare the appearance with Fig. 2. Courtesy of E. Kolmhofer and H. Raab, Ulysses Comet Watch.

The overall morphology of comet Hyakutake's plasma tail confirms the effects of the solar wind on a comet tail as seen in de Vico and other comets. In the equatorial region, a comet's plasma tail is buffeted by the rapidly varying solar wind and numerous kinks, knots, and waves are produced. These deformations are easily observed and produce the "disturbed" appearance as shown in Figs. 2 and 3. As the comet leaves the equatorial region and enters the polar region, the solar wind picks up speed, but the irregularities diminish. Under these conditions, the ions flow downstream more smoothly. The plasma tail formed by these ions has few external disturbances, and thus it appears smooth. Figs. 1 and 3 show this behavior.

4. Tail orientation and solar wind speed

A comet's plasma tail does not point directly anti-sunwards. Instead, the tail points in the direction of the total flow at the comet composed of the solar wind itself and the flows due to the comet's motion, i.e. an aberration effect on a windsock (Biermann 1951; Brandt et al., 1972, 1997b). The magnitude of this deflection can be used to estimate the speed of the solar wind at the comet. The direction of

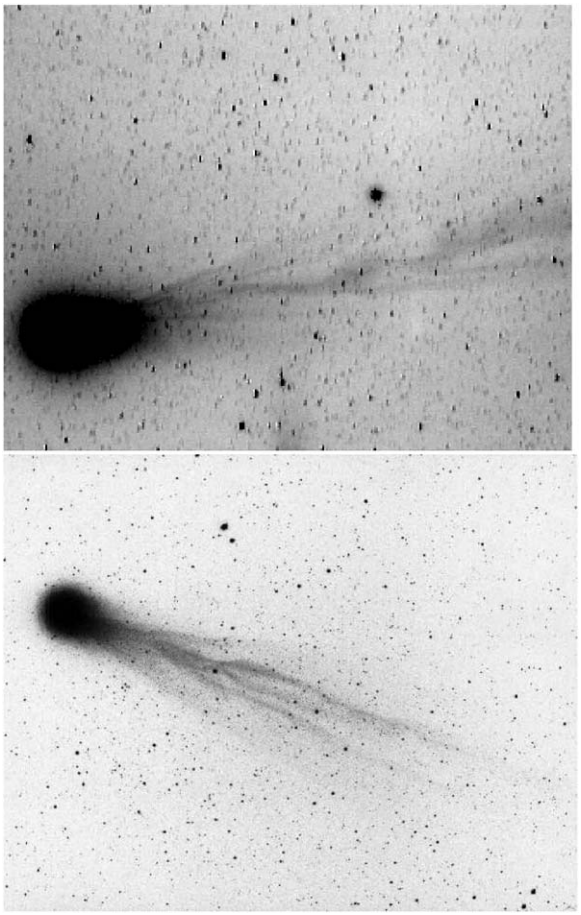

Fig. 2. Images of comet Hyakutake in the equatorial region of the solar wind showing a relatively disturbed appearance. (Top) March 14.25, 1996, latitudes 1°N (ecliptic) and 6°S (heliographic); courtesy of G. Pizarro, European Southern Observatory, La Silla, Chile; (Bottom) March 22.00, 1996 latitudes 4°N (ecliptic) and 3°S (heliographic). Courtesy of J. Drudis, Ulysses Comet Watch. Compare the appearance with Fig. 1.

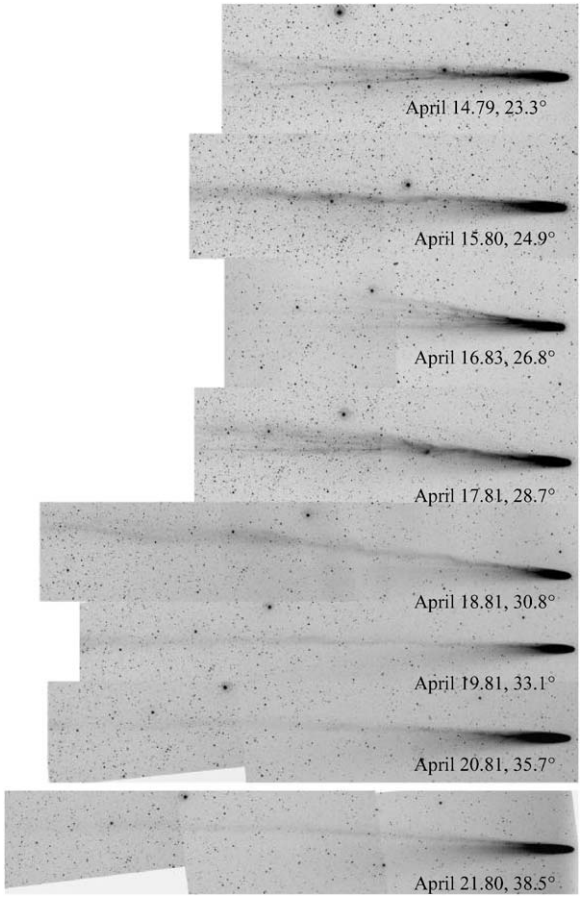

Fig. 3. An eight-day sequence of images showing comet Hyakutake crossing the equatorial–polar solar wind boundary. The images of April 18.8 and earlier appear much more disturbed than the images of April 19.8 and later. This is consistent with an equatorial–polar boundary near 30°N (ecliptic) or 24°N (solar) latitude. Images taken by H. Mikuz, Crni Vrh Observatory, Slovenia and the Ulysses Comet Watch.

the plasma tail is $\mathbf{T} = \mathbf{W} - \mathbf{V}$, where $\mathbf{W}$ is the solar wind velocity and $\mathbf{V}$ is the comet's velocity. Knowing $\mathbf{V}$ from the comet's orbit and measuring the position angle on the sky, Θ the projection of the solar wind velocity on the plane of the sky can be inferred. Brandt et al. (1972) used this technique with many observations taken from a large number of comets to deduce the global solar wind velocity. For observations of a single comet, one must attack the problem from the other direction. If we assume that $\mathbf{W}$ is known, we can calculate the resulting Θ that would be observed. The curves for several assumed values of $\mathbf{W}$ are shown in Fig. 4. Plotting the measured Θ's on these curves gives a rough estimate of the solar wind speed at the comet.

Unfortunately, the observing geometry for comet Hyakutake was not well suited to this technique. The comet came near the Earth, and the Earth passed through the plane of the comet's orbit on March 27th. Measurements of the position angle of the plasma tail do not tightly constrain the solar wind velocity which could have produced the

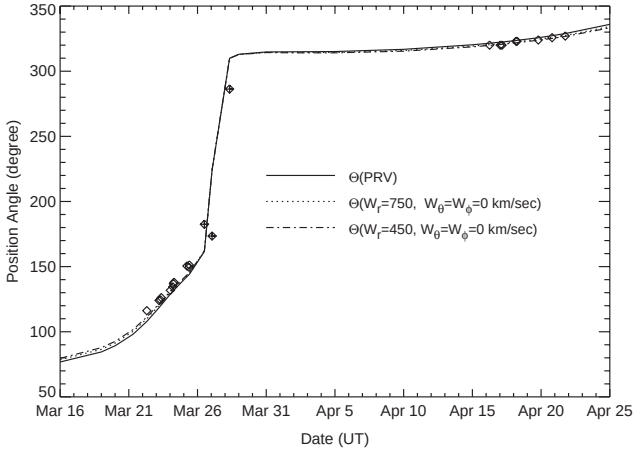

Fig. 4. The observed position angle of comet Hyakutake's plasma tail versus date plotted along with curves for $W_r = \infty$ (the PRV), $W_r = 750$ km s^{-1}, and $W_r = 450$ km s^{-1}. While the points are consistent with the expected behavior, the geometry is not favorable and a firm conclusion is difficult. See Fig. 5 for an alternate presentation of the data and see the text for discussion.

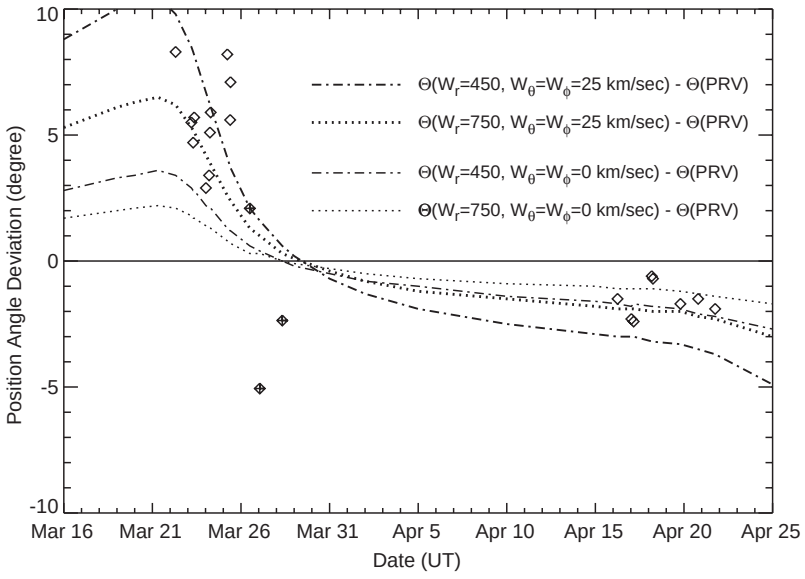

Fig. 5. The observed position angle of comet Hyakutake's plasma tail plotted as the deviation from the position angle for the PRV ($W_r = \infty$). Curves for $W_r = 750$ and 450 km s^{-1} and no non-radial components ($W_\theta = W_\phi = 0$) are plotted along with curves for the same W_r with non-radial components represented by $W_\theta = W_\phi = 25$ km s^{-1}. The points around March 27 (when the earth passed through the plane of the comet's orbit) are plotted with a "+" inside the diamond symbol and have been scaled down by a factor of 10. The points fit the curves with the non-radial component and are generally consistent with the expected pattern. The unfavorable geometry does not allow a solid statement beyond consistency.

deflection shown in Fig. 4. Fig. 5 shows the measured deviation of the position angle from the prolonged radius vector (PRV) direction.

As the solar wind speed increases, the tail points closer to the PRV. This can be seen by considering the angle between the PRV and **T**. For most conditions, this angle is given by $\varepsilon \approx V_\perp/W_r$, where $V_\perp$ is the component of the comet's velocity perpendicular to the PRV and W_r is the radial component of the solar wind. If W_r decreases, the measured deviation in Fig. 5 increases, and vice versa.

As the comet passed the Earth, the position angle of the plasma tail changed very rapidly due to the observing geometry. Observations around March 27th are plotted with a "+" inside the diamond symbol on Figs. 4 and 5. These three observations are from this time of rapid change, and do not fit the curves very well. The deviations of these three points have been scaled down by a factor of 10 in Fig. 5.

We have examined the possibility of a non-radial component to the solar wind and have also plotted its effect on the orientation of the plasma tail in Fig. 5. A relatively small non-radial component of 25 km s^{-1} could have a large impact ($\sim 5°$) on the observed position angle. IMP-8 and solar wind measurements indicate that non-radial velocity components of the magnitude are plausible (see Figs. 6 and 7).

Note in Fig. 5 that the curves with the non-radial component are consistent with the measurements. While the measurements are consistent with the bimodal behavior of the solar wind described in Section 3, they do not constrain the solar wind speed reliably. However, observations in the equatorial region indicate a relatively slower solar wind speed than in the polar region. Unfortunately, a more quantitative estimate of the solar wind speed from these measurements is not possible.

5. Disconnection events

A comet's plasma tail undergoes a multitude of perturbations as it encounters variations in the solar wind. The most spectacular of these phenomena is the DE where the entire plasma tail is severed from the comet's head. Brandt et al. (1999) have shown using 19 such DEs from observations of comet Halley (Brandt et al., 1992, 1997a) that DEs are associated with HCS crossings by the comet at a sector boundary. Yi et al. (1996) (also see Wegmann, 1998; Yi et al., 1998) has established that the physical mechanism which causes a DE is magnetic reconnection in the sunward ionosphere. Thus, DEs should occur only in the equatorial region of the solar wind.

5.1. The spectacular DE of 25 March 1996

Comet Hyakutake was bright and came close to the Earth. It was extensively observed by members of the Ulysses Comet Watch and other observers, and came while the solar wind was measured by IMP-8 and WIND. Thus, the prospects for an excellent, well-documented DE were good and the comet did not disappoint us.

5.1.1. Observations of the DE

This DE may be the most famous DE yet observed. It was featured on the cover of Sky & Telescope magazine for July 1996 and extremely well documented by observers

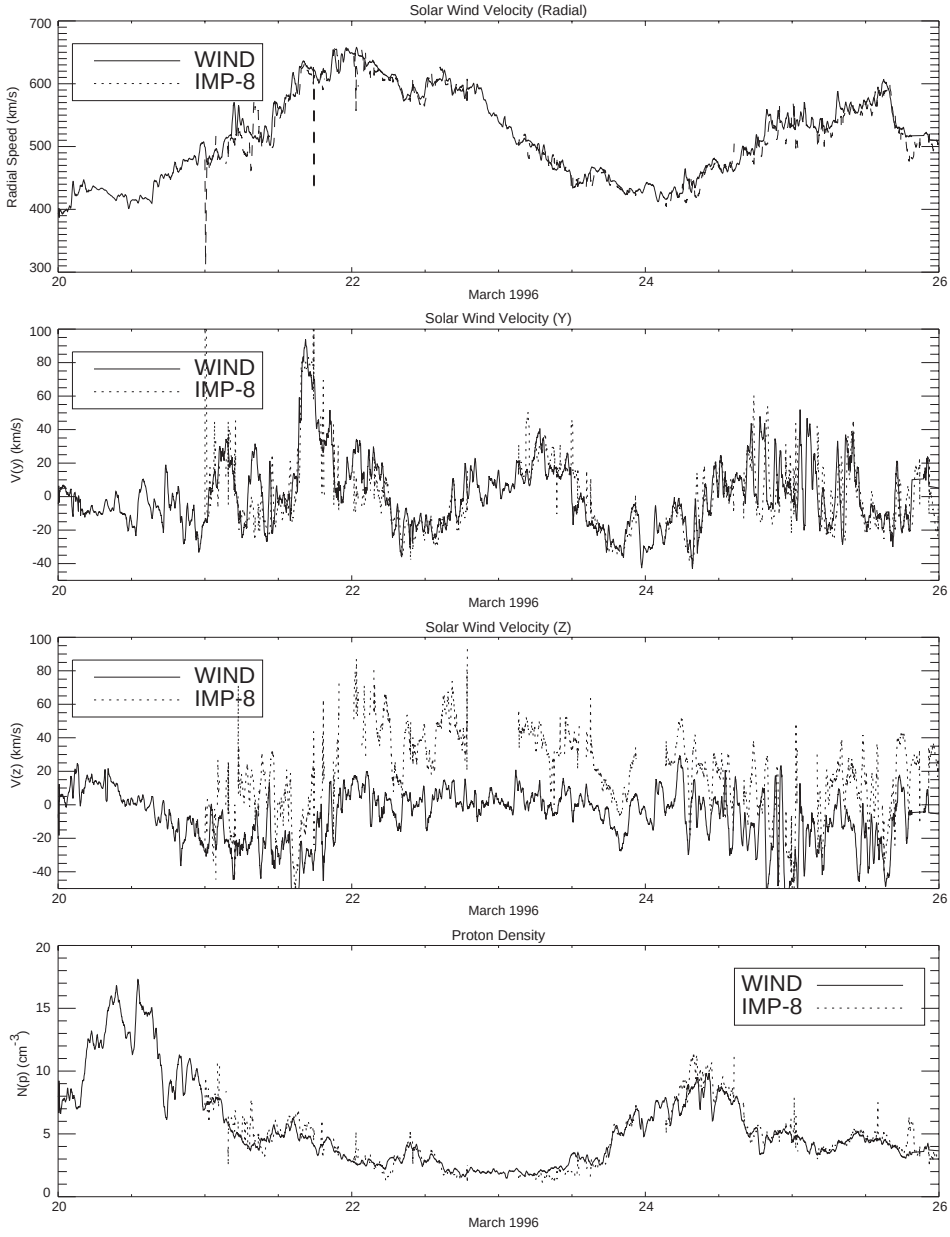

Fig. 6. Solar wind velocity and density measurements from the IMP-8 and WIND spacecraft for the time period March 20–25, 1996. These data show that non-radial solar wind speeds (here labeled as V_y and V_z) of 25 km s^{-1} are plausible. The solid line represents data from WIND. IMP-8 data are represented by the dashed line. Both datasets have been smoothed (insert description here). Data from CDAWeb.

around the world. We have reduced a subset of the available images. Fig. 7 shows the measured recession distance vs. time for the images noted in Appendix A. Sample images are shown in Fig. 8. A parabolic curve fit to these observations produces an estimated disconnection time of March 24.6 (with $v_0 = 21$ km s^{-1} and $a_0 = 49$ cm s^{-2}). The time of disconnection as shown in Fig. 7 is well determined with an estimated uncertainty of 0.1 day.

Kinoshita et al. (1996) studied this DE using observations obtained on March 25, 1996. The distance of the DE from the comet's head varied from approximately 4.9 to 6.8 million km. These observations are well outside the range of distances presented in Fig. 7, and are comparable to the distance for the March 25.74 observation (Fig. 8), and are well within the distance for the March 26.66 observation (Fig. 8). The results from these two investigations are consistent with one exception. Our value for the time of disconnection of March 24.6 uses many observations close to the head and should be preferred to the time of March 24.0 obtained by Kinoshita et al. (1996).

5.1.2. Solar wind plasma measurements

The close passage of comet Hyakutake to Earth (see below) means that the solar wind encountering the comet

may have been sampled by Earth-orbiting spacecraft. Figs. 9 and 10 show the solar wind magnetic field measured by the IMP-8 and WIND spacecraft. Observations from these spacecraft presented here were obtained from the CDA web page (http://cdaweb.gsfc.nasa.gov) and used with permission of the instrument teams.

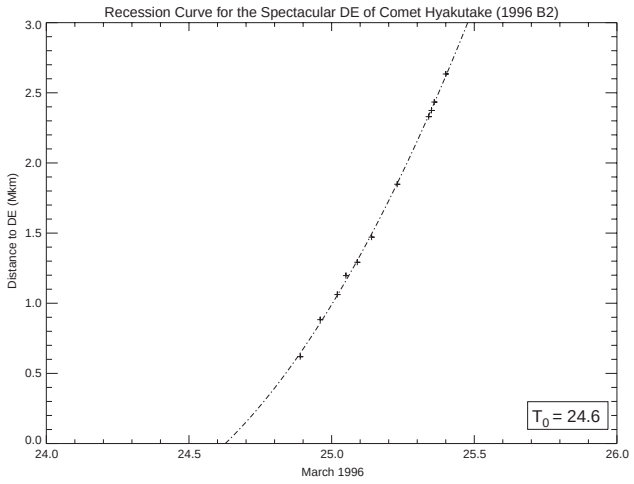

Fig. 7. Recession distance versus time for comet Hyakutake's Great DE. The DE locations are assumed to be along the PRV and the observations are listed in Appendix A. The time of disconnection is March 24.6 with an estimated uncertainty of 0.1 days.

Previous studies of DEs (Niedner and Brandt 1978; Brandt et al., 1999) have indicated that there is a delay of approximately 0.75 days between the time that the comet encounters the magnetic field reversal and the time of disconnection. However, Brandt et al. (1999) presented evidence that the dispersion of this value is about 0.5 days. The time-delay for the solar wind to travel the 0.068 AU from Earth to the comet at 450 km s^{-1} is 0.26 days. Thus, we are interested in the solar-wind conditions as measured for the time period of March 23.1 to 24.1. Because the solar wind as measured by IMP-8 and WIND for the time period earlier than March 24.00 showed a low-magnetic field in the y and z directions (the components that would be captured by the comet), the build-up of the field for the previous polarity could be small and the time of interest is probably close to the later time.

There is unfortunately a data gap in the IMP-8 record at about this time, but the WIND spacecraft detected a significant reversal in the "y" (or azimuthal) component of the magnetic field near the expected time.

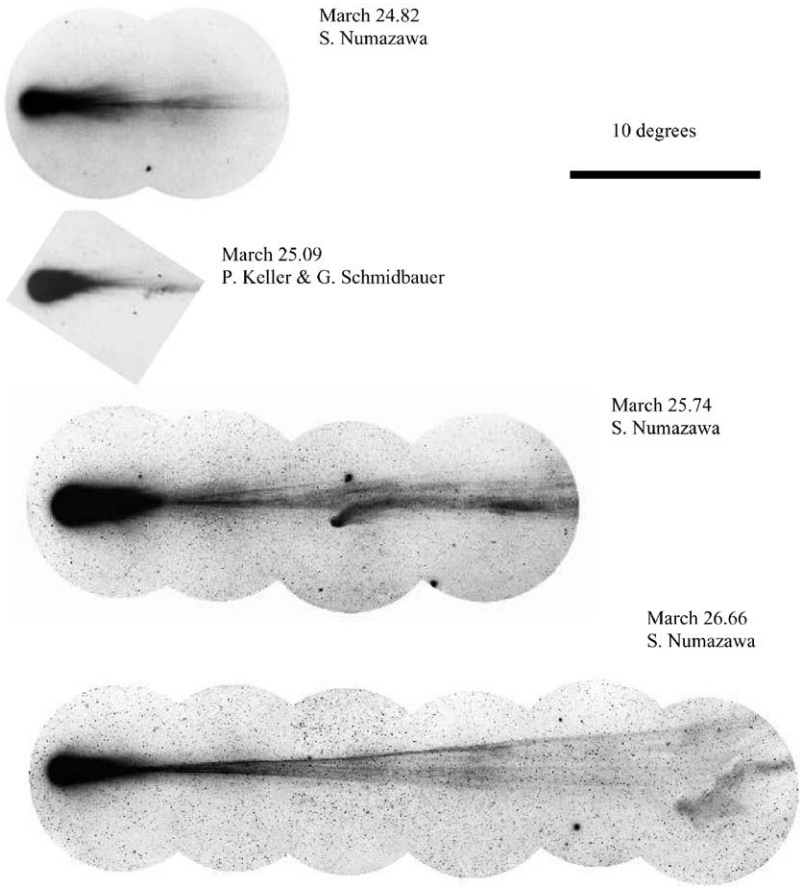

Fig. 8. The Spectacular DE of March 1996 in comet Hyakutake. Top to Bottom: (1) March 24.82; (2) March 25.09, Courtesy of P. Keller and G. Schmidbauer, Ulysses Comet Watch; (3) March 25.74; (4) March 26.66. Note the angular scale indicating 10°. Images (1), (3), and (4) appeared on the cover of *Sky & Telescope* for July 1996. These images Courtesy of *Sky & Telescope* and S. Numazawa, Japan.

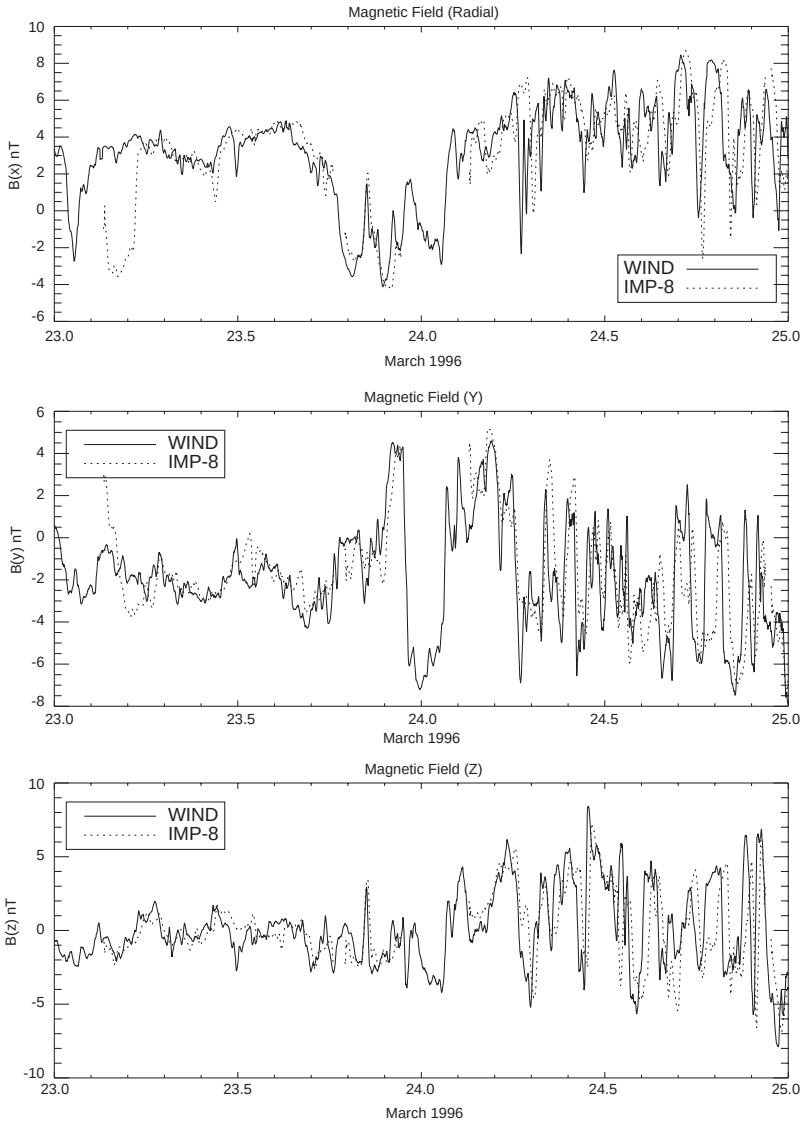

Fig. 9. WIND and IMP-8 measurements of the solar-wind magnetic field for March 23 through March 25, 1996. The solid line shows the data from WIND, the dashed line is from IMP-8. Both datasets have been smoothed as in Fig. 6. Data from CDAWeb.

The candidate reversal is seen to begin at approximately March 23.95. Although the feature seen in Fig. 11 is not the only polarity reversal, it is the dominant feature in the relevant time span with the field being reversed for about 2.5 h, and is possibly responsible for the DE. We examine the assumption that the same solar wind hit the Earth and the comet below.

5.1.3. Geometry and dimensions of the candidate reversal

The candidate reversal in the solar-wind magnetic field lasted for about 2.5 h. At 450 km s^{-1}, this constitutes a region approximately 4 million km thick. There is no definitive study on the minimum duration or thickness of an IMF reversal that can produce a DE. In terms of the theoretical experience available (Yi et al., 1996), we consider this region to be large enough to produce the DE, if this region encountered the comet.

The geometry of the Earth and comet Hyakutake are plotted in Fig. 10. On the scale of the diagrams, WIND and IMP-8 are essentially at Earth. While comet Hyakutake was relatively close to Earth and the spacecraft, the difference in positions in the direction perpendicular to the ecliptic (the z direction), is approximately 13.5 million km. Thus, the candidate region would need to have a height (or z extent) much greater than the thickness (or x extent) in order to have encountered the comet. While possible, this situation seems unlikely and we do not consider this case further.

5.2. Possible causes of the disconnection event

For many other observed DEs, the nature of the reversal in the interplanetary magnetic field (IMF) has been established (cf. Brandt et al., 1999). For the case of the comet Hyakutake

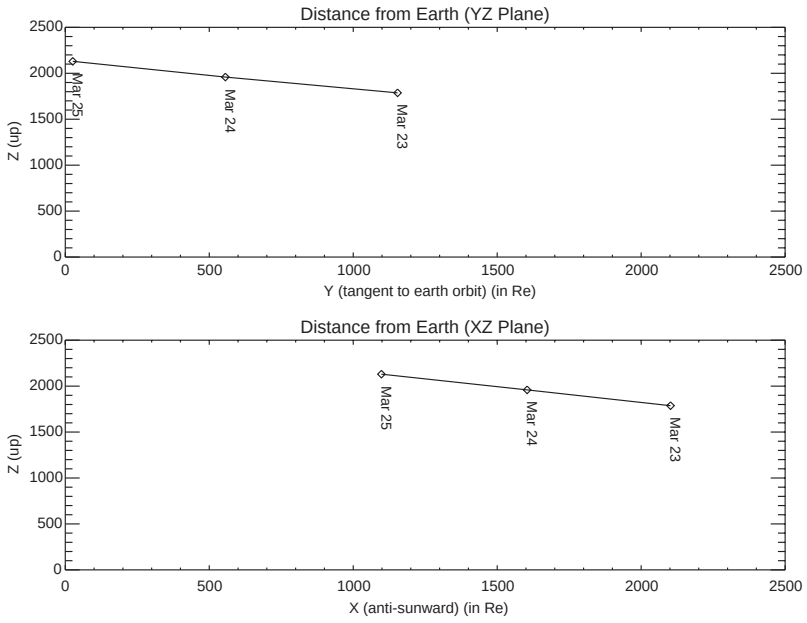

Fig. 10. Geometry of comet Hyakutake and Earth for March 23–25, 1996. On these scales, the IMP-8 and WIND spacecraft are essentially at Earth. The x coordinate is anti-sunward, y is tangent to the earth's orbit, and z is perpendicular to the earth's orbital plane.

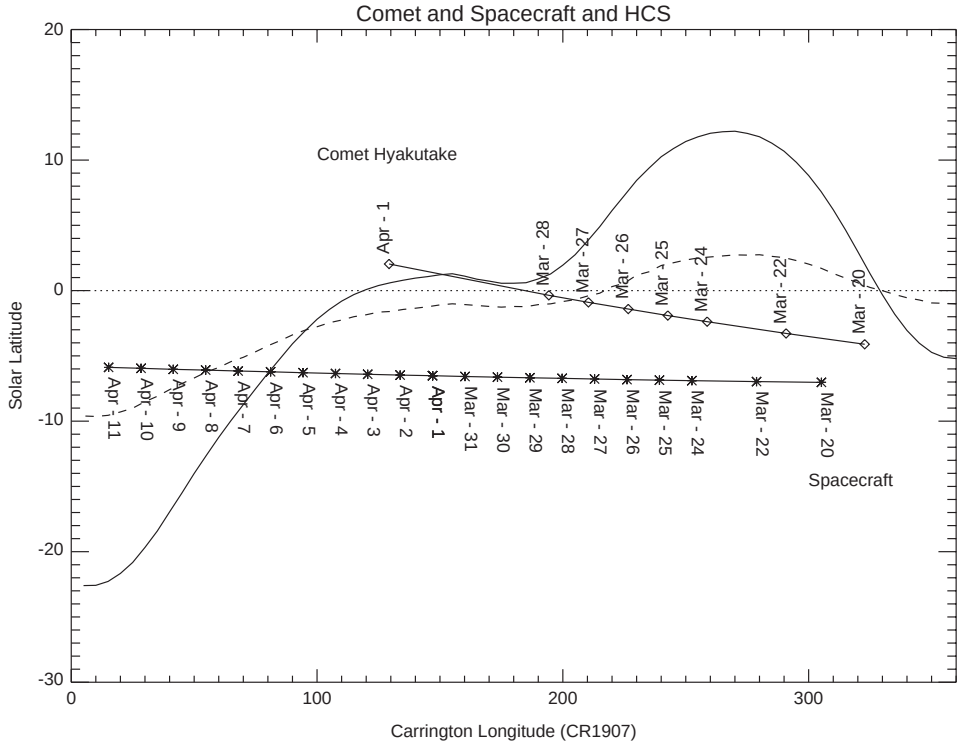

Fig. 11. The Carrington–Niedner diagram for comet Hyakutake around the time of the Great DE showing the positions of the comet, spacecraft, and the HCS; see Yi et al. (1994), and Brandt et al. (1999) for details on the construction of this diagram. The solid curve is the "classic" computation, and the dashed curve is the "radial" computation described in the text.

DE, it occurs in the equatorial region of the solar wind, reasonably close to the HCS, as expected. We examine a list of possible causes and discuss the likelihood of each below. Our conclusion follows the individual discussions.

5.2.1. HCS

The location of the calculated HCS with respect to comet Hyakutake is shown in Fig. 11. The comet is approximately 4–12.5° south of the expected HCS position on March 25.0,

1996. The two values for this distance come about because we have included two different computed HCS curves from the Wilcox Solar Observatory web page. The solid curve is the "classic" computation which locates the source surface at $2.5R_s$, assumes that the photospheric field has a meridional component, and uses an ad hoc polar field correction to match the IMF at the earth. The dashed curve is the "radial" computation which assumes that the magnetic field in the photosphere is radial. According to the Wilcox Solar Observatory web page, "the $R_s = 2.5$ radial model is probably the preferred choice overall". We present the HCS calculated both ways to provide some estimate of uncertainties in the two calculated positions and as a caution against taking calculated positions too seriously.

Brandt et al. (1999) showed that the uncertainty in calculated HCS position compared to spacecraft measurements during the comet Halley interval in 1985 and 1986 was about 5° and was 8–11° for DEs depending on the details. Thus, the distance from the calculated position of the HCS is quite reasonable. In Fig. 11, the calculated HCS curves cross the ecliptic on April 6 and 7. The HCS is clearly shown in the WIND and IMP-8 data on approximately April 6.3, 1996, as expected.

5.2.2. Waves/structure in HCS

The HCS has been known for years to be typically more complex than a simple, smooth boundary. Behannon et al. (1981) studied the boundary structure as observed by Helios 1 and suggested that multiple traversals of the HCS were caused by local fluctuations which, in turn, could be caused by waves or corrugations with scale lengths in the range 0.05–0.10 AU. Suess et al. (1995) discusses the boundary structure in terms of multiple current sheets around an average position and attributes these to eddies in the solar-wind flow. An alternate view has been suggested by Crooker et al. (1993). They attribute the boundary structure to a network of extended current sheets from helmet streamers in the corona. Outflows, such as CMEs (see Gosling (1996) for an excellent review), tend to occur along the HCS and could account for a variety of observed signatures.

The circumstances here are similar to the solar wind encountering Halley's comet in April 1986 (Yi et al., 1993), i.e. a complex magnetic structure. The result in comet Halley was to produce multiple DEs with similar kinematics. In comet Hyakutake, the complex magnetic structure may be responsible for the disturbed, DE-like appearance in the equatorial region as shown in Fig. 2, and the possible DE visible on March 22 (cf. Section 5.3).

5.2.3. Isolated magnetic reversal

Photospheric magnetic field maps from the Wilcox Solar Observatory show an isolated reversal at Carrington longitude ~ 240° (CR 1907 and 1908) and latitude 7.5°N. If this feature could propagate to Earth, it might be responsible for the DE. However, it does not appear in the source surface diagram and the in situ measurements (Figs. 9 and 10) offer little support for this idea.

5.2.4. Transient events

The proximity of the comet to IMP-8 and WIND enables us to investigate possible transient events, e.g. CMEs and shocks, with some confidence. The geometry around the time of the DE is shown in Fig. 10. While it is conceivable that a transient feature could encounter comet Hyakutake and *not* encounter either IMP-8 or WIND, that circumstance is not likely for a major transient.

Solar-wind velocity and density measurements are plotted in Figs. 6 and 7. During the time for the DE, i.e., around March 24.0, the speed is about 425 km s^{-1} and slowly varying. The density is about 8 cm^{-3}. There is no evidence in the spacecraft observations for a significant transient event.

We note that this spectacular DE in comet Hyakutake does not support the suggestion by Wegmann (1995) that some DEs can be produced by shocks, or by high-speed streams or density enhancements (Wegmann, 2000). See Fig. 7.

5.3. Possible DE of 22 March 1996

Coverage of comet Hyakutake on March 22 was sparse and does not allow unequivocal identification of a possible DE or an accurate determination of the time of disconnection. Fig. 12 shows an image of a possible DE taken on March 22.75 by S. Numazawa, Japan. The appearance of the comet tail on this image strongly resembles a DE. If the structure shown on March 22.75 had the same recession curve as for the March 25 DE (the solar-wind conditions are similar; see Fig. 7), T_0 occurred at approximately March 22.2.

An image taken at the Kiso Observatory, University of Tokyo, Japan on March 22.8, 1996 shows the same appearance as Figure 14. With only one exception, we have not found any other images in the time period March 22.2 to 22.8 that could show the possible DE. The exception is an

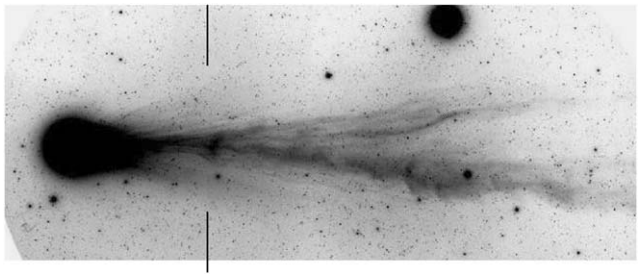

Fig. 12. Possible DE in comet Hyakutake, March 22.75, 1996, courtesy of S. Numazawa, Japan. Tick marks have been added at the top and bottom of the image to mark the forward edge of the possible DE.

image taken by G. Emerson, Ulysses Comet Watch, on March 22.3. Unfortunately, based on the recession curve in Fig. 7, the tip of the DE would be too close to the nucleus and not be visible because of the coma.

There may have been a DE on March 22, 1996. The geometrical circumstances, see Fig. 11, are not much different with respect to the HCS from March 22.2 to March 24.6. This DE could easily have been produced by the HCS or structures associated with it. We also note that the appearance of the comet was quite disturbed before the DE occurred, see Fig. 2.

5.4. Summary of comet Hyakutake DE results

The spectacular DE of March 25, 1996 occurred close to the HCS (Fig. 11) and the general location of the HCS was verified by spacecraft measurements on April 6, 1996. No shocks or high-speed streams were seen in the spacecraft measurements for March 23 and March 24, 1996 (Fig. 7). The density in this interval does not exceed $N_e = N_p = 10$ cm^{-3}. The velocity is approximately 500 km s^{-1} or less in this interval. Therefore, we can consider that this DE was produced by crossing the HCS or current sheet structures associated with the HCS (Niedner and Brandt 1978; Yi et al., 1996; Brandt et al., 1999). A possible DE on March 22, 1996 was briefly described. Fig. 7 shows the solar-wind conditions for March 20 through March 25. The speed exceeds 600 km s^{-1} near March 22.0 and the density exceeds 15 cm^{-3} near March 20.5. These are unrelated to the DE of March 25, but may be relevant for the possible DE of March 22.

6. Conclusion

The overall appearance of comet Hyakutake's plasma tail is consistent with what we know of the solar-wind conditions. In the equatorial region, the plasma tail appears disturbed, suffers DEs, and is oriented consistent with expectations. In the polar region, the plasma tail appears smooth and undisturbed, and no DEs are observed. The orientation at high latitudes is consistent with a steady high-velocity solar wind. Observational coverage of the comet was generally excellent, and we have provided a representative sample here to document the plasma tail's large-scale appearance.

Acknowledgements

We would like to thank all the contributors to the Ulysses Comet Watch. We would also like to thank the MFI and SWE instrument teams on the WIND spacecraft for kindly making their data available to us. We acknowledge the data provider, R. Lepping at NASA/GSFC and CDAWeb. We thank Jon Giorgini, Jet Propulsion Laboratory, for assistance with calculations using the Horizons Ephemeris Generator. This research was partially supported by JPL Grant 959349 to John C. Brandt as an Interdisciplinary Scientist on the *Ulysses* Project.

Appendix A.

Grand table of images reproduced in figures or used in the kinematic analysis.

Date (1996)	R (AU)	Ecliptic Latitude	Heliographic Latitude	Observer	Notes
Mar 14.25	1.27	0.5	−6.2	G. Pizarro	Fig. 2
Mar 22.00	1.11	3.6	−3.3	J. Drudis	Fig. 2
Mar 22.75	1.10	3.9	−2.9	S. Numazawa	Fig. 14
Mar 24.82	1.05	4.9	−2.0	S. Numazawa	Fig. 9
Mar 24.89	1.05	4.9	−2.0	M. Uberti	Fig. 8
Mar 24.96	1.05	4.9	−1.9	M. Uberti	Fig. 8
Mar 25.02	1.05	5.0	−1.9	E. Kolmhofer and H. Raab	Fig. 8
Mar 25.05	1.05	5.0	−1.9	M. Mobberly	Fig. 8
Mar 25.09	1.05	5.0	−1.9	P. Keller and G. Schmidbauer	Figs. 8, 9
Mar 25.14	1.05	5.0	−1.8	P. Keller and G. Schmidbauer	Fig. 8
Mar 25.23	1.05	5.1	−1.8	J. Debusier	Fig. 8
Mar 25.34	1.05	5.1	−1.7	R. Bolster	Fig. 8
Mar 25.35	1.05	5.1	−1.7	W. Brown	Fig. 8
Mar 25.36	1.05	5.2	−1.7	F. Burger	Fig. 8
Mar 25.40	1.05	5.2	−1.7	F. Burger	Fig. 8
Mar 25.74	1.03	5.3	−1.5	S. Numazawa	Fig. 9
Mar 26.66	1.01	5.8	−1.1	S. Numazawa	Fig. 9
Apr 14.79	0.57	23.3	16.0	H. Mikuz	Fig. 3
Apr 15.80	0.55	24.9	17.7	H. Mikuz	Fig. 3
Apr 16.83	0.52	26.8	19.6	H. Mikuz	Fig. 3
Apr 17.81	0.50	28.7	21.4	H. Mikuz	Fig. 3
Apr 18.81	0.47	30.8	23.6	H. Mikuz	Fig. 3
Apr 18.82	0.47	30.9	23.7	E. Kolhmofer and H. Raab	Fig. 1
Apr 19.81	0.45	33.1	25.9	H. Mikuz	Fig. 3
Apr 20.81	0.42	35.7	28.5	H. Mikuz	Fig. 3
Apr 20.81	0.42	35.7	28.5	E. Kolhmofer and H. Raab	Fig. 1
Apr 21.80	0.40	38.5	31.3	H. Mikuz	Fig. 3

References

Behannon, K.W., Neubauer, F.M., Barnstorf, H., 1981. Fine-scale characteristics of interplanetary sector boundaries. J. Geophys. Res. 86, 3273–3287.

Biermann, L., 1951. Kometenschweife und Solar Korpuskularstrahlung. Z. Astrophys. 29, 279–286.

Brandt, J.C., Snow, M., 2000. Heliospheric latitude variations of properties of cometary plasma tails: a test of the Ulysses Comet Watch paradigm. Icarus 148, 52–64.

Brandt, J.C., Roosen, R.G., Harrington, R.S., 1972. Interplanetary gas. XVII. An astrometric determination of solar-wind velocities from orientations of ionic comet tails. Astrophys. J. 177, 277–284.

Brandt, J.C., Niedner Jr., M.B., Rahe, J., 1992. The International Halley Watch Atlas of Large-Scale Phenomena. LASP, University of Colorado, Boulder.

Brandt, J.C., Niedner Jr., M.B., Rahe, J., 1997a. The International Halley Watch Atlas of Large-Scale Phenomena: Supplement 1997. LASP, University of Colorado, Boulder.

Brandt, J.C., Yi, Y., Petersen, C.C., Snow, M., 1997b. Comet de Vico (122P) and latitude variations of plasma phenomena. Planet. Space Sci. 45, 813–819.

Brandt, J.C., Caputo, F.M., Hoeksema, J.T., Niedner Jr., M.B., Yi, Y., Snow, M., 1999. Disconnection events (DEs) in Halley's comet 1985–1986: the correlation with crossings of the heliospheric current sheet (HCS). Icarus 137, 69–83.

Crooker, N.U., Siscoe, G.L., Shodhan, S., Webb, D.F., Gosling, J.T., Smith, E.J., 1993. Multiple heliospheric current sheets and coronal streamer belt dynamics. J. Geophys. Res. 98, 9371–9381.

Gloeckler, G., Geiss, J., Schwadron, N.A., Fisk, L.A., Zurbuchen, T.H., Ipavich, F.M., von Steiger, R., Balsiger, H., Wilken, B., 2000. Interception of comet Hyakutake's ion tail at a distance of 500 million kilometers. Nature 204, 576–578.

Gombosi, T.I., Hansen, K.C., DeZeeuw, D.L., Combi, M.R., Powell, K.G., 1997. MHD simulation of comets: the plasma environment of comet Hale–Bopp. Earth Moon Planets 79, 179–207.

Gosling, J.T., 1996. Corotating and transient solar wind flows in three dimensions. Ann. Rev. Astron. Astrophys. 34, 35–73.

Jones, G., Balogh, A., Horbury, T., 2000. Identification of comet Hyakutake's extremely long ion tail from magnetic field signatures. Nature 404, 574–576.

Jones, G.H., 2002. Ulysses encounter with Comet Hyakutake. In proceedings of Asteroids, Comets, Meteors (ACM 2002), ESA SP-500, pp. 563–566.

Kinoshita, D., Fukushima, H., Watanabe, J.-I., Yamamoto, N., 1996. Ion tail disturbance of comet C/Hyakutake 1996 B2 observed around the closest approach to the Earth, Publ. Astron. Soc. Japan, 48, L83–L86 (and plate 21).

McComas, D.J., Bame, S.J., Barraclough, B.L., Feldman, W.C., Funsten, H.O., Gosling, J.T., Riley, P., Skoug, R., Balogh, A., Forsyth, R., Goldstein, B.E., Neugebauer, M., 1998. Ulysses return to the slow solar wind. Geophys. Res. Lett. 25, 1–4.

McComas, D.J., Elliott, H.A., Gosling, J.T., Reisenfeld, D.B., Skoug, R.M., Goldstein, B.E., Neugebauer, M., Balogh, A., 2002. Ulysses' second fast-latitude scan: complexity near solar maximum and the reformation of polar coronal holes. Geophys. Res. Lett. 29(9) 10.1029/2001GL014164.

Niedner Jr., M.B, Brandt, J.C., 1978. Interplanetary Gas. XXIII. Plasma tail disconnection events in comets: evidence for magnetic field line reconnection at interplanetary sector boundaries. Astrophys. J. 223, 655–670.

Phillips, J.L., Bame, S.J., Barnes, A., Barraclough, B.L., Feldman, W.C., Goldstein, B.E., Gosling, J.T., Hoogeveen, G.W., McComas, D.J., Neugebauer, M., Suess, S.T., 1995a. Ulysses solar wind plasma observations from pole to pole. Geophys. Res. Lett. 22, 3301–3304.

Phillips, J.L., Bame, S.J., Feldman, W.C., Goldstein, B.E., Gosling, J.T., Hammond, C.M., McComas, D.J., Neugebauer, M., Scime, E.E., Suess, S.T., 1995b. Ulysses solar wind plasma observations at high southerly latitudes. Science 268, 1030–1033.

Sky and Telescope, Cover, July 1996.

Smith, E.J, et al., 2001. Ulysses in the South Polar Cap at solar maximum: heliospheric magnetic field. Geophys. Res. Lett. 28, 4159–4162.

Suess, S.T., McComas, D.J., Bame, S.J., Goldstein, B.E., 1995. Solar wind eddies and the heliospheric current sheet. J. Geophys. Res. 100, 12261–12273.

Wegmann, R., 1995. MHD model calculations for the effects of interplanetary shocks on the plasma tail of a comet. Astronaut. Aeronaut. 294, 601–614.

Wegmann, R., 1998. Comment on "Global MHD simulation of a comet crossing the HCS" by Yi, Walker, Ogino, & Brandt. J. Geophys. Res. 103, 6633–6635.

Wegmann, R., 2000. The effect of some solar wind disturbances on the plasma tail of a comet: models and observations. Astron. Astrophys. 358, 759–775.

Yi, Y., Brandt, J.C., Randall, C.E., Snow, M., 1993. The Disconnection events of 1986 April 13–18 and the cessation of plasma tail activity in comet Halley in 1986 May. Astrophys. J. 414, 883–891.

Yi, Y., Caputo, F.M., Brandt, J.C., 1994. Disconnection events (DEs) and sector boundaries: the evidence from comet Halley 1985–1986. Planet. Space Sci. 42, 705–720.

Yi, Y., Walker, R.J., Ogino, T., Brandt, J.C., 1996. Global magnetohydrodynamic simulation of a comet crossing the heliospheric current sheet. J. Geophys. Res. 101, 27585–27601.

Yi, Y., Walker, R.J., Ogino, T., Brandt, J.C., 1998. Reply. J. Geophys. Res. 103, 6637–6639.